02

^{15}N isotope enrichment of the atomic nitrogen component in atomic-molecular exchange reactions in the post-discharge zone

© S.V. Gudenko,[1,2] N.M. Gorshunov[1]

[1] National Research Center „Kurchatov Institute“, Moscow, Russia
[2] Moscow Institute of Physics and Technology, Dolgoprudny, Moscow oblast, Russia
e-mail: svgudenko@gmail.com

Received August 6, 2021
Revised November 28, 2021
Accepted December 21, 2021

A kinetic model is presented that explains the more than thirty-fold enrichment of the atomic nitrogen component with the ^{15}N isotope in the post-discharge zone. Isotopic enrichment is due to the activation nature of the exchange reaction of atoms with vibrationally excited nitrogen molecules, the upper vibrational levels of which are enriched with molecules containing a heavier isotope during non-equilibrium vibrational-vibrational exchange. The dependences of the concentrations of ^{14}N and ^{15}N atoms on the time of nitrogen flow through a quartz tube emerging from the region of a pulsed electric discharge are obtained. In addition to exchange, the model took into account the dissociation of molecules, the recombination of atoms, and the loss of the vibrational energy of molecules on the surface of the tube. The obtained dependence of the increase in the ratio of the concentrations of ^{15}N to ^{14}N atoms on the time of nitrogen flow through the post-discharge zone satisfactorily describes the experimental data published earlier and obtained in this work.

Keywords: Trinor distribution, gas excitation regime, inverse population.

DOI: 10.21883/TP.2022.04.53598.232-21

Introduction

Nitrogen isotope ^{15}N is used widely as a tracer in various ecological, agrochemical, pharmacological, and biological studies (specifically, in studies into the protein metabolism of humans and farm livestock; see, e.g., reviews [1–4]). The interest in ^{15}N has been on the rise in recent years in relation to the projects of fast power reactors with nitride fuel (U, Pu)N. Nitride fuel has the following advantages: high density, high thermal conductivity, and compatibility with the primary materials of fuel-element cladding and liquid-metal coolants (sodium and lead). However, nitrogen isotope ^{14}N, which accounts for 99.7% of naturally occurring nitrogen, is converted under the influence of reactor neutrons into long-lived radioactive carbon isotope ^{14}C that has a negative effect on the neutron physics of nitride fuel and leads to excessive gas release. The mentioned drawbacks of nitride fuel may be eliminated by substituting natural nitrogen with nitrogen enriched with ^{15}N [5,6]. In view of this, the issue of development of methods for production of low-cost isotope ^{15}N is a fairly relevant one. The development of a method for separation of nitrogen isotopes based on the effect of a multifold increase in the relative concentration of isotope ^{15}N in the atomic nitrogen component flowing along a tube emerging from the region of an electrical discharge may be a step toward solving the mentioned issue. This is the effect considered in the present study.

It is known that electrons in an electrical discharge in nitrogen excite a large number of vibrational and electronic-vibrational levels of molecules N_2 and cause the dissociation of molecules. In the near afterglow region, the energy accumulated at excited electronic-vibrational levels is rapidly released or quenched in collisions and is converted into the vibrational energy of the ground electronic state of N_2 ($X^1\Sigma_g^+$). Therefore, when nitrogen flows through the discharge region and the afterglow region, vibrationally excited molecules of the ground electronic state and atoms are the species most likely to be found in the post-discharge zone. Electrons (at least those capable of inducing dissociation and excitation of electronic levels of nitrogen molecules) do not penetrate beyond the afterglow region. When moving within the post-discharge zone, vibrationally excited molecules may maintain a nonequilibrium state, where the effective vibrational temperature remains considerably higher than the rotational and translational temperatures, for up to several seconds. Within this time interval, the populations of vibrational levels of anharmonic molecules are characterized by the quasi-equilibrium Trinor distribution [7], which turns into a slightly sloping decreasing plateau at levels with a high vibrational energy, instead of the Boltzmann function. The upper vibrational levels are much more populated in this case than under the equilibrium Boltzmann distribution with the same vibrational energy reserve [8,9].

In a mixture of isotopic modifications of molecules (e.g., $^{1414}N_2$ and $^{1415}N_2$) with nonequilibrium vibrational exchange, the upper levels of the Trinor distribution and the plateau region are populated primarily by the heavy

isotopic modification [10]. Thus, $^{1415}N_2$ molecules gain an advantage in terms of crossing the energy threshold of chemical reactions and in dissociation. The possibility of application of nonequilibrium vibrational exchange in separation of isotopes in the course of chemical reactions has been reported for the first time in [11]. A tenfold enrichment of the atomic nitrogen component with ^{15}N was observed in subsequent EPR (electron paramagnetic resonance) experiments in nitrogen that flowed over a distance of 37 cm along a quartz tube from the microwave discharge region to the center of the EPR spectrometer cavity. The magnitude of enrichment decreased rapidly as impurity oxygen was added to the flow of nitrogen [12]. In our previous study [13], the isotopic composition of nitrogen atoms was also determined by EPR spectroscopy, but the velocity of nitrogen flow along a quartz tube connecting the region of a pulsed electrical discharge to the EPR spectrometer cavity was varied. It turned out that a more than 30-fold isotopic enrichment is obtained at lower flow velocities. This implies that the primary region of enrichment of the atomic component with isotope ^{15}N is the post-discharge zone (and not the electrical discharge itself). Two probable mechanisms of enrichment of the atomic component were examined qualitatively in [13]. It was assumed in the first one that enrichment is attributable to the reactions of dissociation of vibrationally excited molecules and atomic–molecular exchange reactions, which mostly involve the molecules on high vibrational levels of the ground electronic state. The second mechanism was a complex process of two-stage enrichment involving electronically excited states ($A^3\Sigma_u^+$ and $B^3\Pi_g$). A phenomenological dependence of the enrichment coefficient on time was derived for this mechanism. However, a consistent kinetic model explaining how atomic enrichment coefficients of this magnitude are achieved has not been developed.

1. Problem formulation and details of the experiment

The aim of the present study is to identify the mechanism of a more than thirty-fold enrichment of the atomic nitrogen component with isotope ^{15}N in the post-discharge zone of a pulsed discharge and develop a kinetic model that illustrates consistently how the relative concentrations of atoms ^{15}N and ^{14}N vary in the course of flow of excited gas along a quartz tube and how this variation depends on the degree of vibrational excitation of gas; its density and temperature; the rates of dissociation of molecules, vibrational relaxation of molecules, and recombination of atoms on tube walls; and the atomic–molecular exchange rate. The atomic–molecular exchange has not been taken into account in numerical simulations and analytical studies of isotopic effects in an electrical discharge in earlier research [9,10,14]. Upon close examination, it was found that the mechanism of two-stage enrichment involving electronically excited states ($A^3\Sigma_u^+$ and $B^3\Pi_g$), which was proposed in our study [13], is not capable of altering the isotopic composition of the atomic component in a gas flow through the post-discharge zone in any significant way, since the mentioned states have relatively low populations and lifetimes. The relative population of these states under excitation conditions close to those set in our study was no higher than $1 \cdot 10^{-6}$, and the lifetimes did not exceed $1 \cdot 10^{-4}$ s [15–17], while the fraction of dissociated non-enriched molecules in our experiments was always higher than $1 \cdot 10^{-4}$, and the time of nitrogen flow through the post-discharge zone exceeded $1.5 \cdot 10^{-2}$ s.

The theoretical model of isotopic enrichment of atoms in the course of flow of excited gas through the post-discharge zone was developed based on our experimental data (the majority of which were published in [13]). In the present study, the results from [13] were combined with the needed additional data that were also obtained in these experiments but had not been reported. In addition, new experimental results corresponding to longer times of nitrogen flow along the measurement tube were obtained, and the EPR spectra were processed once again, this time more thoroughly (the ranges of background measurement and line integration were expanded). This is the reason why the experimental data on enrichment presented below differ somewhat from those reported in [13]. Let us detail the key conditions of the experiment that need to be borne in mind when characterizing the considered theoretical model.

Nitrogen flowed through the pulsed discharge region, where various vibrational and electronic levels of nitrogen molecules were populated under electron bombardment, and molecules were dissociated partially. High-purity nitrogen (99.999; first grade according to GOST 9293-74) was fed into a discharge quartz tube with inner diameter $d_{ch} = 0.7$ cm and length $L_{ch} = 21$ cm. Electrical discharge was produced by a pulsed voltage generator upon self-breakdown of a capacitor to gas in the tube. The discharge time was around $2\,\mu$s, the interpulse interval was $30-100$ ms, and the breakdown voltage was several kV. The average power transferred to a single molecule of gas in a discharge, W_T, depended on the energy stored in the capacitor, the pulse frequency, and the flow of nitrogen molecules and varied within the range of $W_T \cong 250-750\,\mathrm{eVs^{-1}mol^{-1}}$. The wall temperature of the discharge tube was kept close to $T_{ch} = 400$ K throughout the experiment with the use of air cooling. Nitrogen from the discharge tube flowed into a quartz measurement tube with inner diameter $d = 1.5$ cm that ran through the cavity of an EPR spectrometer. The distance from the discharge tube outlet to the center of the cavity was $L = 20$ cm. Valves adjusting the flow of nitrogen were used to keep the pressure in tubes constant throughout the experiment within the range from 333 to 733 Pa (2.5–5.8 Torr). The measurement tube temperature was kept close to $T = 300$ K. Atoms of ^{14}N and ^{15}N were identified in the flow of partially dissociated nitrogen by their EPR signal. Nitrogen molecules do not contain uncompensated electron spins and produce no contribution to the EPR signal. Spin I of nuclei of nitrogen atoms

induces hyperfine splitting of EPR lines of ^{14}N ($I = 1$) atoms into three components, while the lines of ^{15}N ($I = 1/2$) atoms are split into two components. The first magnetic-field derivative of the absorption signal at a frequency of 9.535 GHz was measured. Since the typical spectrum recording time was no shorter than 10−15 min (i.e., exceeded considerably the interval between generator pulses), the probable perturbations of the EPR signal due to fluctuations of average discharge power W_T in the course of gas flow along the discharge tube (at high flow velocities) were smoothed out. The ratio of concentrations of ^{15}N and ^{14}N atoms in the nitrogen flow through the spectrometer cavity was determined by comparing the results of double integration of the obtained lines. The spectrometer was calibrated against the EPR signal of molecular oxygen [18,19] to determine the absolute concentrations of ^{14}N and ^{15}N atoms. This allowed us to estimate molecule dissociation degree $\delta = {}^{14}N/(2{}^{1414}N_2)$ (here and elsewhere, the concentrations of atoms ^{14}N, ^{15}N and molecules $^{1414}N_2$, $^{1415}N_2$, N_2 are denoted by the same symbols in cursive). In our experiments, this dissociation degree fell within the $1 \cdot 10^{-4} < \delta < 2 \cdot 10^{-2}$ range. The dependence of coefficient $\beta_A = ({}^{15}N/{}^{14}N)/(\beta_{0M}/2)$ of enrichment of the atomic nitrogen component with isotope ^{15}N on time t of nitrogen flow along the measurement tube to the center of the cavity was obtained as a result of measurements ($\beta_{0M} = {}^{1415}N_2/{}^{1414}N_2 = 2/273$ is the natural ratio of concentrations of molecules $^{1415}N_2$ and $^{1414}N_2$). Time t was set by varying the gas flow rate and the corresponding gas velocity v in the measurement tube:

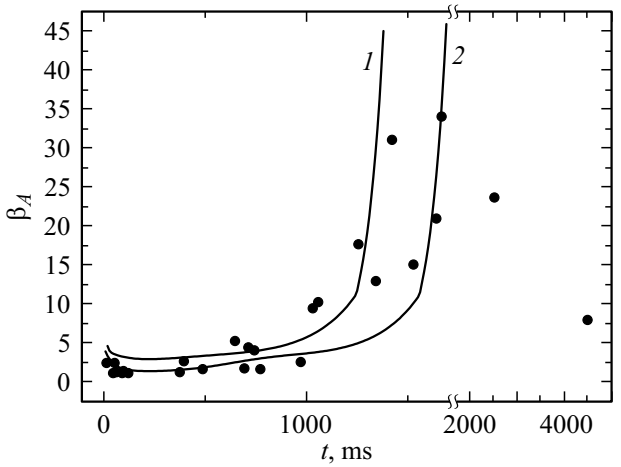

Figure 1. Experimental data on the dependence of coefficient $\beta_A(t)(\bullet)$ of enrichment of the atomic nitrogen component on the time of flow through the post-discharge zone at $T \cong 300$ K and an average total power per a molecule in the discharge of $W_T \cong 250-750\,\mathrm{eVs^{-1}mol^{-1}}$. Approximating curves were plotted in accordance with functions (21), (47), (49) with the use of relations (28), (38), (39) for $T = 300$ K, $T_{ch} = 400$ K, time of vibrational energy deactivation $\tau_M = 270$ ms, and the following values of the vibrational energy pumping power per a single molecule: $W = 70\,\mathrm{eVs^{-1}mol^{-1}}$ (curve *1*) and $W = 210\,\mathrm{eVs^{-1}mol^{-1}}$ (curve *2*).

$t = L/v$. The experimental results are presented in Fig. 1. It can be seen that enrichment coefficient β_A tends to increase in the interval up to $t \cong 1700$ ms from several units at $t < 1000$ ms to several tens at 1300 ms $< t <$ 1700 ms. The maximum value is $\beta_A^{\max}(1667\,\mathrm{ms}) = 34$. Experimental points $\beta_A^{\max}(2530\,\mathrm{ms}) = 23.6$ and $(4500\,\mathrm{ms}) = 7.9$, which indicate that the coefficient of atomic enrichment decreases as the flow time increases further, are also plotted in Fig. 1.

2. Results and discussion

Vibrationally excited molecules and atoms, which were produced as a result of partial dissociation of molecules under the influence of a discharge, flow from the discharge tube to the post-discharge zone in the measurement tube. The primary processes occurring in the measurement tube are the loss of vibrational energy of molecules as a result of deactivation on tube walls and vibrational–translational ($V-T$) relaxation, the dissociation of vibrationally excited molecules, the recombination of atoms on tube walls, and the atomic–molecular exchange. Let us consider the example of nitrogen and see how the concentration of ^{14}N and ^{15}N atoms at given distance L from the post-discharge zone inlet varies in these conditions with time t of flow through this zone.

2.1. Dependence of the vibrational distribution function of diatomic anharmonic nonradiative molecules on the degree of gas excitation

As will be shown below, the degree of gas excitation and the corresponding average vibrational energy of molecules are defined by the intensity of a pulsed discharge and the times of gas flow along the discharge and post-discharge tubes. Let us examine how the distribution of molecules over vibrational levels is affected by variations of the degree of gas excitation. With only the vibrational–vibrational ($V-V$) exchange taken into account, the population distribution of anharmonic diatomic molecules with vibration quantum $k_B E_1$, anharmonicity $\gamma = \Delta E_1/E_1$, and energy levels

$$k_B E_n = k_B E_1 \{n[1 - \gamma(n-1)] + 0.5\} \qquad (1)$$

over vibrational levels n is characterized by the Trinor formula [7,8]:

$$f^{Tr}(n) = f(0) \exp\left\{-nE_1\left[\frac{1}{T_1} - \frac{\gamma(n-1)}{T}\right]\right\}. \qquad (2)$$

Here, T is the translational temperature, parameter $T_1 = E_1/\ln[f(0)/f(1)]$ is the vibrational temperature of the first level, k_B is the Boltzmann constant, and parameter E_1 characterizes the vibration quantum energy in degrees Kelvin. The Trinor distribution has a minimum at

$$n_0 = (T/2\gamma T_1) + 0.5. \qquad (3)$$

The value corresponding to it is

$$f^{Tr}(n_0) = f(0)\exp(-n_0^2\gamma E_1/T). \quad (4)$$

Note that Eq. (3) allows one to rewrite the expression for the Trinor distribution in the following form:

$$f^{Tr}(n) = f(0)\exp\left\{[(n-n_0)^2 - n_0^2]\gamma E_1/T\right\}. \quad (5)$$

2.1.1. Weak excitation mode In real-world systems, the processes of vibrational–translational ($V-T$) relaxation and the probable chemical reactions (e.g., dissociation) are crucial for highly excited states. When the deviation from equilibrium is small and the populations of highly excited levels are low, the nonresonance $V-V$ exchange of molecules in these states with molecules in lower vibrational states is dominant, and the Trinor distribution is established only for levels with $n < n_W$, where level n_W for nonradiative molecules is defined by the following expression [8]:

$$n_W = (\delta_{VV} + \delta_{VT})^{-1} \ln\left[\frac{3Q_{10}^{01}\left(1-\exp(-E_1/T)\right)}{2P_{10}\left(1-\exp(\delta_{VV}-E_1/T)\right)^2}\right]. \quad (6)$$

Here, Q_{10}^{01} and P_{10} are the rate constants of $V-V$ exchange and $V-T$ relaxation between the first and the zeroth levels per a single collision (in the case of nitrogen at $T = 300\,\mathrm{K}$, constants $Q_{10}^{01} = 9\cdot10^{-15}\,\mathrm{cm^3 s^{-1}}$ and $P_{10} = 8\cdot10^{-22}\,\mathrm{cm^3 s^{-1}}$ [20]) and δ_{VT} and δ_{VT} are the factors characterizing the exponential dependence of rate constants of $V-V$ exchange and $V-T$ relaxation on the numbers of vibrational levels. In a single-component gas, these factors are equal: $\delta_{VV} = \delta_{VT} = 0.427\gamma E_1\sqrt{\mu/T}/\lambda$, where λ is the constant in exponential repulsive potential $U \propto \exp(-\lambda r)$ of intermolecular interaction (in $\mathrm{Å^{-1}}$) and μ is the reduced mass of colliding particles (in a.m.u.). In the case of nitrogen, $\lambda = 4\,\mathrm{Å^{-1}}$ [21], $\mu = 14$, $^{1414}E_1 = 3345\,\mathrm{K}$, $\gamma = 6.22\cdot10^{-3}$ [22], and $\delta_{VV} = \delta_{VT} = 0.48$ at $T = 300\,\mathrm{K}$.

The probabilities of $V-T$ processes start exceeding the probabilities of $V-V$ exchanges as the level number increases at $n > n_W$, and Boltzmann distribution

$$f^{B}(n) \propto \exp(E_n/T) \quad (7)$$

is established with translational gas temperature T. In accordance with (6), the value of n_W depends relatively weakly on T_1. For example, n_W for nitrogen at $T = 300\,\mathrm{K}$ changes from 17.31 to 17.68 (i.e., only slightly) as T_1 varies from 610 to 1850 K, while the position of minimum n_0 of the Trinor distribution shifts from 40 to 13.5. Equality $n_W = n_0 = 17.5$ is established at $T_1 = 1419\,\mathrm{K}$. This implies that $n_W < n_0$ at $T_1 < 1419\,\mathrm{K}$, and the Trinor distribution changes to Boltzmann distribution (7) without reaching its minimum; at $T_1 > 1419\,\mathrm{K}$, $n_W > n_0$ and inverse population of vibrational levels is possible in the $n > n_0$ region. The intermediate excitation mode (see below) sets in here. Figure 2 shows the calculated functions of distribution of nitrogen molecules $^{1414}N_2$ over vibrational levels at translational temperature $T = 300\,\mathrm{K}$ for different excitation modes.

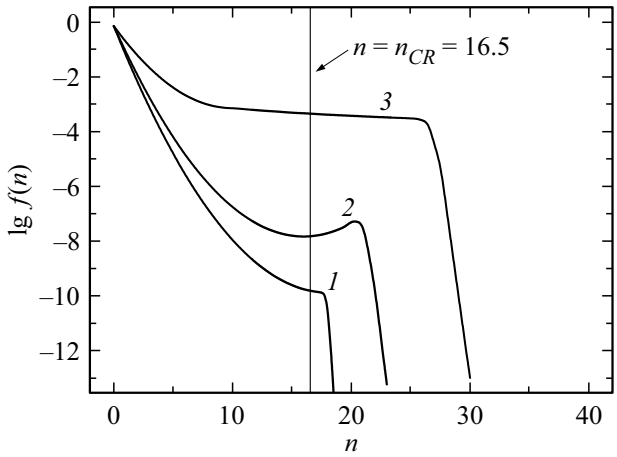

Figure 2. Calculated functions of distribution of nitrogen molecules $^{1414}N_2$ over vibrational levels at translational temperature $T = 300\,\mathrm{K}$ for different excitation modes. Curve *1* corresponds to weak excitation at $T_1 = 1378\,\mathrm{K}$ and the corresponding value of $n_0 = 18$. Curve *2* represents intermediate excitation at $T_1 = 1555.9\,\mathrm{K}$ and the corresponding value of $n_0 = 16$. Curve *3* corresponds to strong excitation at $T_1 = 2538.5\,\mathrm{K}$ and the corresponding value of $n_0 = 10$. The value of $n = n_{CR} \cong 16.5$, above which the atomic–molecular exchange reaction is activated, is also indicated.

Curve *1* corresponds to weak excitation at $T_1 = 1318\,\mathrm{K}$ and the corresponding value of $n_0 = 18$. The transition from the Trinor distribution to the Boltzmann one at this temperature occurs at $n = n_W = 17.56 < n_0 = 18$.

2.1.2. Strong excitation mode When the deviation from equilibrium is large ($T \ll T_1 \approx E_1$ and the populations of highly excited levels are significant), collisions and the exchange with a small resonance defect between molecules in these states play a pivotal role. As was demonstrated in [8], the Trinor distribution is preserved in this case up to $n = n_0$, and a slowly decreasing sloping plateau with

$$f(n) \approx f^{Tr}(n_0)(n_0+1)/(n+1), \quad (8)$$

which stretches to a certain boundary value of $n = n_P$, forms afterwards. The distribution at higher n values decreases rapidly in a Boltzmann exponential fashion with gas temperature T. In the case of nonradiative molecules, the plateau region is bounded primarily by the ratio between the rates of $V-V$ exchange and $V-T$ relaxation:

$$n_P \cong \delta_{VT}^{-1} \ln\left[f^{Tr}(n_0)(n_0+1)\frac{Q_{10}^{01}}{P_{10}}\frac{12\gamma E_1\delta_{VT}}{T\delta_{VV}^3} + \exp(\delta_{VT}n_0)\right]. \quad (9)$$

The mode of large deviation from equilibrium is established when the following inequality is fulfilled [23]:

$$\frac{n_0+1}{\delta_{VV}}\exp\left(-\frac{n_0^2\gamma E_1}{T}-0.5\right)>\left[1-\exp\left(\delta_{VV}-\frac{E_1}{T_1}\right)\right]^{-2}\times\exp\left(-\frac{E_1}{T_1}-n_0\delta_{VV}\right). \quad (10)$$

In the case of nitrogen at $T=300\,\mathrm{K}$, the solution of (10) yields $T_1>0.6E_1\cong 2007\,\mathrm{K}$, which corresponds to $n_0<12.5$. Curve *3* in Fig. 2 represents the strong excitation mode at $T=300\,\mathrm{K}$, $T_1=2538.5\,\mathrm{K}$ and the corresponding value of $n_0=10$. The transition from the Trinor distribution to the plateau occurs at $n=n_0=10$, and the plateau itself extends, in accordance with (9), to $n=n_P=27$. Boltzmann distribution (7) with translational temperature $T=300\,\mathrm{K}$ is established at higher n values.

2.1.3. Intermediate excitation mode As was already noted, the examined modes of large and small deviation from equilibrium may exist alongside with the intermediate mode of moderate deviation from equilibrium, which was considered in [8,24], in the $17.5>n_0\geq 12.5$ region. Just as in the large deviation mode, a slightly sloping plateau is produced in the intermediate mode due to the resonance $V-V$ exchange; however, this plateau starts forming not at n_0, but slightly later (at $n=n_I>n_0$). As in the small deviation mode, the distribution at lower values of $n<n_I$ is shaped by the $V-V$ exchange with lower states and is a Trinor one. Inverse population of vibrational levels is established at $n_I>n>n_0$. The equation for n_I was derived in [8]:

$$\exp\left[n_I\left(\delta_{VV}-\frac{\gamma E_1}{T}(2n_0-n_I)\right)\right]=\frac{\eta\delta_{VV}\left(1+\delta_{VV}(n_I-n_0)\right)}{2(n_I+1)}, \quad (11)$$

where parameter

$$\eta=\exp\left(-\frac{2n_0\gamma E_1}{T}\right)\left[1-\exp\left(-\delta_{VV}-\frac{2n_0\gamma E_1}{T}\right)\right]^2. \quad (12)$$

The following estimate of n_I for nitrogen at $T=300\,\mathrm{K}$ may be obtained using Eqs. (11) and (12):
at $13.5\leq n_0\leq 17$,

$$n_I=n_0+\sqrt{[(n_0-11.5)/0.776]^2-6.64}, \quad (13)$$

and n_I varies from 13.5 to 23.6 as n_0 increases within the indicated interval; at $12.5\leq n_0\leq 13.5$, $n_I=n_0$, no inversion is observed, and the distribution has the same form as the one corresponding to a large deviation from equilibrium. The formulae for the distribution function on the plateau and the plateau length in the intermediate mode are similar to formulae (8) and (9) that are valid for the large deviation mode, but n_0 needs to be substituted in them with n_I:

$$f(n)\approx f^{Tr}(n_I)(n_I+1)/(n+1), \quad (14)$$

$$n_{PI}\cong\delta_{VT}^{-1}\ln\left[f^{Tr}(n_I)(n_I+1)\frac{Q_{10}^{01}}{P_{10}}\frac{12\gamma E_1\delta_{VT}}{T\delta_{VV}^3}+\exp(\delta_{VT}n_I)\right]. \quad (15)$$

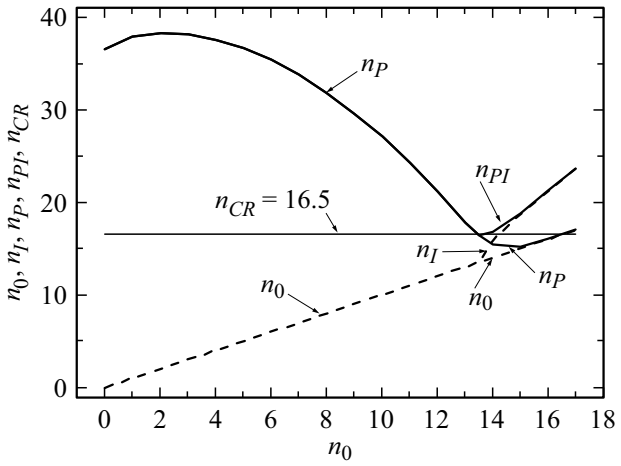

Figure 3. Trinor distribution $n<n_0(n_I)$ and plateau $n_0(n_I)<n<n_P(n_{PI})$ regions for the modes of strong and intermediate excitation of vibrational levels of nitrogen $^{1414}N_2$ at $T=300\,\mathrm{K}$. Functions n_P, n_{PI}, n_I were plotted in accordance with (9), (15), and (13). The value of $n=n_{CR}$, above which the atomic–molecular exchange reaction is activated, is also indicated.

Curve *2* in Fig. 2 represents the intermediate excitation mode at $T=300\,\mathrm{K}$, $T_1=1555.9\,\mathrm{K}$ and the corresponding value of $n_0=16$. The transition from the Trinor distribution to the plateau occurs (13) at $n=n_I=21.1$, and the plateau itself extends, in accordance with (15), to $n=n_{PI}=21.2$ (i.e., degenerates almost to a point). Boltzmann distribution (7) with translational temperature $T=300\,\mathrm{K}$ is established at higher n values.

Figure 3 shows the dependences of n_P, n_{PI}, n_I on n_0 plotted in accordance with (9), (15), and (13) for nitrogen $^{1414}N_2$ at $T=300\,\mathrm{K}$. It can be seen that n_P varies within a wide interval from $n_P=38$ (this is almost the level of dissociation $n_D\approx 42$ [22]) at $n_0=2$ to the minimum of $n_P\cong 15$ at $n_0=15$. Starting at this value ($n_0=15$), n_P becomes almost equal to n_0, and the plateau degenerates into a point. In the inversion region, n_{PI} has a minimum at $n_0=13.5$ and approaches n_I rapidly at $n_0\geq 14.5$, and the plateau also degenerates into a point.

2.2. Molecular enrichment coefficient

The vibrational distribution functions in a binary mixture of diatomic molecular gases in substantially nonequilibrium conditions of strong and intermediate excitation were considered in [10]. If the concentration of one component is significantly higher than the concentration of the other,

${}^{A}N_M \gg {}^{B}N_M$, distribution function ${}^{A}f(n)$ is formed primarily in $A-A$ collisions, and distributions (2), (8), and (14) considered above remain valid for it in the corresponding regions. Distribution function ${}^{B}f(n)$ is formed primarily in $A-B$ collisions, and if the rates of $V-T$ relaxation are low compared to the rates of $V-V$ exchange and anharmonicities are similar ($\Delta^{A}E_1/\Delta^{B}E_1 \cong 1$):
(a) in the Trinor distribution region $n \le n_0 - m_0$ ($n \le n_I - m_0$), where $m_0 = ({}^{A}E_1 - {}^{B}E_1)/(2\Delta^{A}E_1)$, it is also a Trinor one (2), but with temperature ${}^{B}T_1$ determined using the following relation:

$$ {}^{A}E_1/{}^{A}T_1 - {}^{B}E_1/{}^{B}T_1 = ({}^{A}E_1 - {}^{B}E_1)/T; \qquad (16) $$

(b) in the plateau region $n_P > n > n_0 - m_0$ ($n_{PI} > n > n_I - m_0$), it „repeats“ the ${}^{A}f(n)$ function with a shift by a certain number of levels

$$ {}^{B}f(n) \cong C_B {}^{A}f(m_0 + n\Delta^{B}E/\Delta^{A}E), \qquad (17) $$

where constant C_B is determined using the $\sum\limits_n {}^{B}f(n) = 1$ normalization condition (physically, this stems from the fact that ${}^{B}f(n)$ forms in resonance processes of quanta exchange between molecules A and B, and, as follows from (1), the equality of quanta at equal anharmonicities ${}^{A}\gamma = {}^{B}\gamma$ corresponds to the following relation between level numbers: ${}^{A}n = m_0 + {}^{B}n\Delta^{B}E/\Delta^{A}E$). Using (2), (8), (14), (16), and (17), we obtain the following for the molecular enrichment coefficient [10]:

$$ \beta_M(n) \equiv \frac{{}^{B}f(n)}{{}^{A}f(n)} \cong \exp\left(\frac{{}^{A}E_1 - {}^{B}E_1}{T}\, n\right) = \exp\left(\frac{{}^{A}E_1(\alpha - 1)}{\alpha T}\, n\right) \qquad (18) $$

at $n \le n_0 - m_0$ ($n \le n_I - m_0$) and

$$ \beta_M(n) \cong \exp\left[({}^{A}E_1 - {}^{B}E_1)\big(2n_0(n_I) - m_0\big)/(2T)\right] = \exp\left[{}^{A}E_1(\alpha - 1)\big(n_0(n_I) - (\alpha - 1)/(4\gamma_A\alpha)\big)/(\alpha T)\right] \qquad (19) $$

at $n_P > n > n_0$ ($n_{PI} > n > n_I$). Here, the ratio of magnitudes of vibrational quanta of molecules A and B is denoted as $\alpha = {}^{A}E_1/{}^{B}E_1$.

The natural ratio of concentrations of molecules ${}^{1415}N_2$ and ${}^{1414}N_2$ for nitrogen is $\beta_{0M} \ll 1$, and condition ${}^{A}N_M \gg {}^{B}N_M$ is well satisfied. In addition, the value of $\alpha = {}^{A}E_1/{}^{B}E_1 = 1.0171$ is just slightly above unity. If anharmonicities are equal (${}^{1414}\gamma = {}^{1415}\gamma$), which is a fairly natural corollary of the fact that molecules with different isotopes have the same electronic structure, this implies that ratio $\Delta^{1414}E_1/\Delta^{1415}E_1 = \alpha$ is also close to unity. It follows from the above that formulae (18) and (19) are applicable to nitrogen. It can be seen from these formulae that since ${}^{1414}E_1 > {}^{1415}E_1$, the heavier component is subject to enrichment, and the degree of enrichment increases exponentially with level number in the Trinor distribution region and levels off in the plateau region.

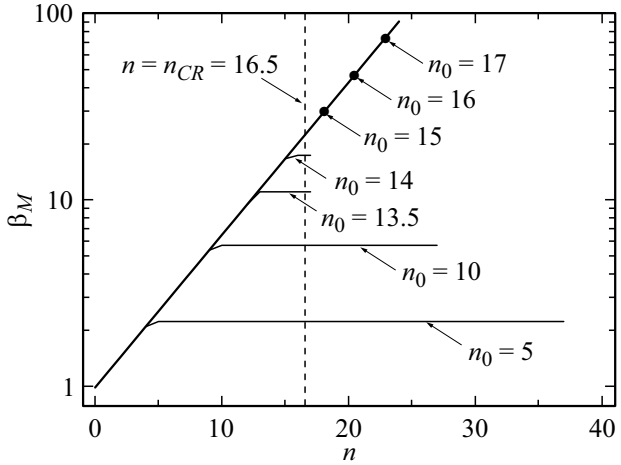

Figure 4. Dependences of molecular enrichment coefficient $\beta_M(n) \equiv {}^{1415}f(n)/{}^{1414}f(n)$ on vibrational level number n at certain values of n_0. The curves were plotted in accordance with (20) and (21) for nitrogen at $T = 300$ K. Symbol • denotes the limit values of coefficient β_M at $n_0 = 15$, 16, 17 when the plateau degenerates into a point.

Formulae (18) and (19) for nitrogen at $T = 300$ K are written as

$$ \beta_M(n) \cong \exp(n/5.33) \qquad (20) $$

in the Trinor distribution region at $n \le n_0 - 1.35$ ($n \le n_I - 1.35$) and

$$ \beta_M(n) \cong \exp\left[\big(n_0(n_I) - 0.675\big)/5.33\right] \qquad (21) $$

in the plateau region at $n_P > n > n_0$ ($n_{PI} > n > n_I$).

Figure 4 shows the dependences of the molecular enrichment coefficient on level n at certain values of n_0 plotted in accordance with (20) and (21) in the corresponding regions of n. It can be seen that the enrichment coefficient on the plateau increases with n_0, while the plateau itself shrinks (see above) and degenerates into a point at $n_0 \ge 14.5$. The maximum value of molecular enrichment coefficient $\beta_M \cong 74$ is achieved at the boundary of the inverse population region for $n_0 \cong 17$ at $n \cong 23.6$.

2.3. Atomic enrichment coefficient

2.3.1. Dependence of the average vibrational energy of molecules on the time of gas flow through the post-discharge zone Average vibrational energy ε of molecules and vibrational temperature T_1 decrease in the process of deactivation of the vibrational energy of molecules on walls and as a result of vibrational–translational relaxation. The characteristic setting time of the local vibrational temperature in a particle ensemble may be estimated in terms of rate constant Q_{10}^{01} of $V-V$ exchange and molecule concentration N_2: $\tau_{VV} \approx (Q_{10}^{01}N_2)^{-1}$. In the case of nitrogen at $T = 300$ K with concentration $N_2 \approx 1 \cdot 10^{17}\,\mathrm{cm}^{-3}$ (this corresponds to a pressure of around 3 Torr), $\tau_{VV} \approx 1 \cdot 10^{-3}$ s. The characteristic time

of $V-T$ relaxation of molecules at each other may be estimated in terms of rate constant P_{10} of vibrational–translational relaxation: $\tau_{VT} \approx (P_{10}N_2)^{-1}$. In the case of nitrogen in the same conditions, $\tau_{VT} \approx 1 \cdot 10^4$ s. As was noted in [9,25,26], the rate constant of $V-T$ relaxation of molecules at atoms may be considered, as a first approximation, comparable to the rate constant of $V-T$ relaxation at molecules, but, in view of the smallness of dissociation degree $\delta = {}^{14}N/(2^{1414}N_2)$ (in our experiments, $1 \cdot 10^{-4} < \delta < 2 \cdot 10^{-2}$; see above) and the activation nature of the atomic–molecular exchange (molecules on high levels $n > n_{CR} \cong 16.5$ are primarily involved in it; see below), its influence on the resulting rate of $V-T$ relaxation of molecules may be neglected.

Characteristic time $\tau_{DR} \approx R^2/D$ of radial diffusion at tube radius $R = 0.75$ cm and diffusion coefficient $D \approx 50\,\mathrm{cm^2 s^{-1}}$ corresponding to the considered gas concentration and temperature is $\tau_{DR} \approx 1 \cdot 10^{-2}$ s. It is evident that $\tau_{VV} \ll \tau_{DR}$. If it also turns out that characteristic time τ_M of deactivation of the vibrational energy of molecules on walls is much longer than these times and much shorter than times $\tau_{DL} \approx L^2/D$ and τ_{VT} of longitudinal diffusion, one may derive the equation characterizing the deactivation process kinetics by examining the motion with the flow velocity of a designated gas volume on the order of R^3 with average vibrational energy of molecules $\varepsilon(t)$ and vibrational temperature $T_1(t)$ varying smoothly with time. The equation for $\varepsilon(t)$ assumes the following form in these conditions:

$$\frac{d\varepsilon}{dt} = -\frac{\gamma_M v_M}{2R}(\varepsilon - \varepsilon_{T_1=T}) \equiv -\frac{\varepsilon - \varepsilon_{T_1=T}}{\tau_M}, \qquad (22)$$

and its solution is

$$\varepsilon(t) = \varepsilon_{T_1=T} + (\varepsilon_{ch} - \varepsilon_{T_1=T})\exp(-t/\tau_M). \qquad (23)$$

Here, ε_{ch} is the average vibrational energy of molecules at the discharge tube outlet, $\varepsilon_{T_1=T}$ is the average vibrational energy of molecules at $T_1 = T$ immediately after deactivation on the tube surface with temperature $T \cong 300$ K, γ_M is the probability of deactivation of a molecule on tube walls ($\gamma_M \approx 1 \cdot 10^{-4}$ [26,27] for a quartz tube at near-room (and slightly higher) temperatures), and v_M is the average thermal velocity of molecules ($v_M \cong 5 \cdot 10^4\,\mathrm{cm\,s^{-1}}$ at room temperature). The characteristic time of deactivation of the vibrational energy in these conditions is

$$\tau_M = \frac{2R}{\gamma_M v_M} \approx 0.3\,\mathrm{s} \gg \tau_{DR} \approx 1 \cdot 10^{-2}\,\mathrm{s}. \qquad (24)$$

At $L = 20$ cm, the longitudinal diffusion time is $\tau_{DL} \approx 8\,\mathrm{s} \gg \tau_M$, and assumptions

$$\tau_{VT}, \tau_{DL} \gg \tau_M \gg \tau_{DR} \gg \tau_{VV}, \qquad (25)$$

which are needed for Eq. (22) to remain valid, are thus fulfilled.

Let us determine how average vibrational energy of molecules ε_{ch} at the discharge tube outlet depends on time of flow t_{ch} along this tube with length $L_{ch} = 21$ and radius $R_{ch} = 0.35$. As in (22), the variation of energy of molecules is characterized by equation

$$\frac{d\varepsilon_{ch}}{dt_{ch}} = W - \frac{\varepsilon_{ch} - \varepsilon_{T_1=T_{ch}}}{\tau_{chM}}. \qquad (26)$$

Here, W is the average amount of vibrational energy received by a single molecule from the discharge in unit time (pumping power per a single molecule) and $\varepsilon_{T_1=T_{ch}}$ is the average vibrational energy of molecules at $T_1 = T_{ch}$ immediately after deactivation on the discharge tube surface with temperature $T_{ch} \approx 400$ K. The solution of (26) is written as

$$\varepsilon_{ch}(t_{ch}) = \varepsilon_{T_1=T_{ch0}}\exp(-t_{ch}/\tau_{chM}) + (W\tau_{chM} + \varepsilon_{T_1=T_{ch}}) \times [1 - \exp(-t_{ch}/\tau_{chM})], \qquad (27)$$

where $\varepsilon_{T_1=T_{ch0}}$ is the average vibrational energy of molecules at temperature $T_1 = T_{ch0}$ at the discharge tube inlet (T_{ch0} matched fairly accurately the temperature of walls of the post-discharge tube: $T_{ch0} \cong T \cong 300$ K) and $\tau_{chM} \cong \tau_M(R_{ch}/R)\sqrt{T/T_{ch}} \cong 0.4\tau_M$ (see (24)) is the characteristic time of relaxation of vibrational energy on the discharge tube wall. It is easy to verify that the conditions similar to (25), which are needed for Eq. (26) to remain valid, are also fulfilled here (constants $Q_{10}^{01} = 1.4 \cdot 10^{-14}\,\mathrm{cm^3 s^{-1}}$ and $P_{10} = 6 \cdot 10^{-21}\,\mathrm{cm^3 s^{-1}}$ [20] for nitrogen at $T = T_{ch} = 400$ K). It follows from the continuity of gas flow that time t_{ch} of flow along the discharge tube is related to time t of flow along the post-discharge tube in the following way: $t_{ch} = \frac{L_{ch}R_{ch}^2 T}{LR^2 T_{ch}}t = 0.17\,t$. Considering the above, we obtain the following from relations (23) and (27) for the vibrational energy in the measurement tube at the center of the EPR cavity:

$$\begin{aligned}\varepsilon(t) &\cong \varepsilon_{T_1=T} + \Big\{\varepsilon_{T_1=T_{ch0}}\exp(-t_{ch}/\tau_{chM}) - \varepsilon_{T_1=T} \\ &+ (W\tau_{chM} + \varepsilon_{T_1=T_{ch}})\big[1 - \exp(-t_{ch}/\tau_{chM})\big]\Big\}\exp(-t/\tau_M) \\ &\cong \varepsilon_{T_1=T} + (0.4W\tau_M + \varepsilon_{T_1=T_{ch}} - \varepsilon_{T_1=T})\exp(-t/\tau_M) \\ &\times \big[1 - \exp(-0.425t/\tau_M)\big]. \qquad (28)\end{aligned}$$

According to (28), the average vibrational energy of a molecule at a given power W first increases with time of flow through the post-discharge zone, reaches its maximum $\varepsilon_{\max} \cong 0.052W\tau_M$ at $t = t_{\max} = 0.83\tau_M$, and then decreases. This yields $\varepsilon_{\max} \cong 0.98-2.94\,\mathrm{eV\,mol^{-1}}$ at $t = t_{\max} = 225$ ms (Fig. 5) for the characteristic values of $\tau_M = 270$ ms and pumping power $W = 70-210\,\mathrm{eVs^{-1}mol^{-1}}$ (see below) .

2.3.2. Dependence of the concentration of atoms of isotopes ^{14}N and ^{15}N and the atomic enrichment coefficient on the time of gas flow through the post-discharge zone

The reduction in concentration

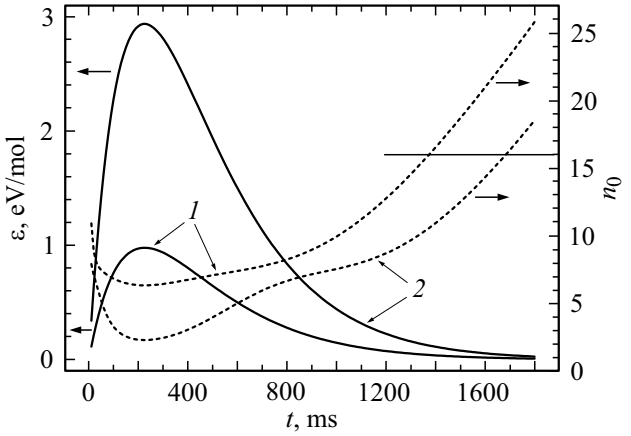

Figure 5. Dependences of average vibrational energy ε (solid curves) and position n_0 of the Trinor distribution minimum (dotted curves) of nitrogen molecules on the time of flow through the post-discharge zone. These curves were plotted using formulae (28) and (38) for $T = 300\,\mathrm{K}$, $T_{ch} = 400\,\mathrm{K}$, $\tau_M = 270\,\mathrm{ms}$, and the following values of the vibrational energy pumping power per a single molecule: $W = 70\,\mathrm{eVs^{-1}mol^{-1}}$ (curves *1*) and $W = 210\,\mathrm{eVs^{-1}mol^{-1}}$ (curves *2*).

of atoms due to their recombination on a tube wall is characterized by equation

$$\left(\frac{d^{14(15)}N}{dt}\right)_R = -\frac{^{14(15)}N}{\tau_A}, \tag{29}$$

which is valid under the constraints on characteristic time τ_A of recombination of atoms on a wall (similar to the constraints set in the case of relaxation of molecules)

$$\tau_{VV} \ll \tau_{DR} \ll \tau_A = \frac{2R}{\gamma_A v_A} \ll \tau_{DL}, \tag{30}$$

and is defined, just as in the case of deactivation of energy on a wall, by tube radius R, thermal velocity v_A of atoms, and reaction probability γ_A. Inserting the typical values for room-temperature conditions and a quartz tube ($v_A \cong 7 \cdot 10^4\,\mathrm{cm \cdot s^{-1}}$, $\gamma_A \approx 3 \cdot 10^{-5}$ [28,29], $R = 0.75\,\mathrm{cm}$), we find $\tau_A \approx 0.7\,\mathrm{s}$. It is evident that $\tau_A \approx \tau_M$ and inequality (30) is well satisfied.

The dissociation rate of vibrationally excited molecules is defined by the dissociation coefficients of the considered molecules ($^{1415}k_D$ and $^{1414}k_D$) and their concentrations ($^{1414}N_2$ and $^{1415}N_2$) [8]. In view of the smallness of $\beta_{0M} \ll 1$, the following is true for the dissociation rates:

$$\left(\frac{d^{14}N}{dt}\right)_D = 2^{1414}k_D(^{1414}N_2)^2 \tag{31}$$

and

$$\left(\frac{d^{15}N}{dt}\right)_D = {}^{1415}k_D^{1415}N_2^{1414}N_2 = {}^{1415}k_D\beta_{0M}(^{1414}N_2)^2. \tag{32}$$

It follows from the results presented in [8] that the dissociation coefficients in the modes of large and moderate deviation from equilibrium may be estimated using formulae

$$^{1414}k_D \approx \frac{2.2Q_{10}^{01}\gamma E_1(n_0+1)^2\left(f^{Tr}(n_0)\right)^2}{n_D\delta_{VV}^2 T}, \tag{33}$$

$$^{1415}k_D \approx \beta_M(n_0)^{1414}k_D, \tag{34}$$

where n_D is the level at which molecular dissociation occurs (as was already noted, $n_D \approx 42$ for nitrogen). Inserting the parameter values for nitrogen into (33) at $T = 300\,\mathrm{K}$, we find

$$^{1414}k_D \approx 3 \cdot 10^{-16}\,\mathrm{cm^3s^{-1}}(n_0+1)^2\left(f^{Tr}(n_0)\right)^2. \tag{35}$$

The contribution of the atomic–molecular exchange to the dynamics of variation of concentrations of ^{14}N and ^{15}N atoms is given by

$$\left(\frac{d\,^{15}N}{dt}\right)_{AM} = -\left(\frac{d\,^{14}N}{dt}\right)_{AM} = {}^{1414}N_2\Big[(^{14}N - {}^{15}N)$$

$$\times\beta_{0M}\sum_0^{n_D}K_n\,{}^{1415}f(n) - 2\,{}^{15}N\sum_0^{n_D}K_n\,{}^{1414}f(n)\Big]. \tag{36}$$

Here, K_n is the rate constant of the atomic–molecular exchange. The process of atomic–molecular exchange is of an activation nature: only molecules on sufficiently high energy levels may be involved in it. Experimental coherent anti-stokes Raman spectroscopy (CARS), Penning ionization, and UV photoelectron spectroscopy studies for nitrogen suggest that the efficiency of relaxation of N_2 molecules on the lower 14 levels in collisions with nitrogen atoms is low. However, the atomic–molecular exchange reaction at levels higher than 20 plays a significant part in dissociation and ionization and may be efficient in deactivation of the vibrational energy of nitrogen molecules ([9]). Exchange rate constant K_n reaches its limiting gas-kinetic value of $K_{CR} \approx 1.5 \cdot 10^{-10}\,\mathrm{cm^3s^{-1}}$ in this case. According to the results of calculations [9], the rate constant of the atomic–molecular exchange in a similar system (boron atoms with vibrationally excited nitrogen molecules) increases by more than 10 orders of magnitude at a translational temperature below 500 K in transition from vibrational level $n = 14$ to $n = 16$. As level number n increases further, the reaction rate constant approaches the rate constant of gas-kinetic collisions. In view of the foregoing, we assume in subsequent estimates that rate constant K_n of the atomic–molecular exchange for nitrogen in the conditions of our study takes on the limiting gas-kinetic value of $K_n = K_{CR} \approx 1.5 \cdot 10^{-10}\,\mathrm{cm^3s^{-1}}$ at $n \geq n_{CR} \cong 16.5$ and tends quickly to a negligible value at $n \leq n_{CR}$.

With such nature of the atomic–molecular exchange, one may set vibrational temperature T_1 (and the corresponding value of n_0 (3)) so that only the molecules on vibrational levels with a considerable degree of enrichment β_M in regions $n_{CR} < n < n_P(n_{PI})$ will be involved in this exchange

(Figs. 3 and 4). The plateau boundary sets the upper bound for the atomic–molecular exchange region, since the concentration of molecules decreases rapidly in a Boltzmann fashion at the end of the plateau (Fig. 2). Therefore, the summation limits in (36) may be restricted to this $(n_{CR} < n < n_P(n_{PI}))$ interval. This will be taken into account below.

The right-hand parts of expressions (31)–(36) are functions of n_0. As was demonstrated in [8], the following approximation is valid for the average vibrational energy per a single molecule in the strong excitation mode:

$$\varepsilon \approx k_B E_1 \Big\{ [\exp(E_1/T_1) - 1]^{-1} + f^{Tr}(n_0)(n_0+1)(n_P - n_0)\exp(-0.5) \Big\}. \quad (37)$$

The first and the second terms in curly brackets characterize the energy reserve corresponding to the Trinor region and the „plateau“region, respectively. The solution of (37) with respect to n_0 with (3), (4), and (9) taken into account yields the following approximating dependence for nitrogen at $T = 300$ K:

$$n_0 \cong 7.21\ln(k_B E_1/\varepsilon + 1) + 0.5 + 630\Big[\exp\big(-\varepsilon/(2.9k_B E_1)\big) - \exp\big(-\varepsilon/(2.85k_B E_1)\big)\Big]. \quad (38)$$

The second term in formula (37) may be neglected in the modes of weak and intermediate excitation at $n_0 > 12.5$, and the expression for n_0 takes the form

$$n_0 \cong 7.21\ln(k_B E_1/\varepsilon + 1) + 0.5. \quad (39)$$

With dependence (28) of average molecule energy $\varepsilon(t)$ on flow time being known, we obtain time dependence $n_0(t)$ (Fig. 5). This provides an opportunity to express the right-hand parts of Eqs. (31)–(36) in the form of functions of time t.

Combining relaxation (29), exchange (36), and dissociation ((31) and (32)) contributions, we derive a system of equations that allows one to determine (with relations (28), (34), (35), (38), and (39) taken into account) the time dependences of concentrations of atoms and atomic enrichment coefficient $\beta_A(t)$:

$$\frac{d^{15}N}{dt} = -\frac{^{15}N}{\tau_A} + {}^{1415}k_D\beta_{0M}(^{1414}N_2)^2 + {}^{1414}N_2\Bigg[(^{14}N - {}^{15}N) \times \beta_{0M}\sum_{n_{CR}}^{n_P(n_{PI})} K_{CR}\,{}^{1415}f(n) - 2{}^{15}N\sum_{n_{CR}}^{n_P(n_{PI})} K_{CR}\,{}^{1414}f(n)\Bigg],$$

$$\frac{d^{14}N}{dt} = -\frac{^{14}N}{\tau_A} + 2{}^{1414}k_D(^{1414}N_2)^2 - {}^{1414}N_2\Bigg[(^{14}N - {}^{15}N) \times \beta_{0M}\sum_{n_{CR}}^{n_P(n_{PI})} K_{CR}\,{}^{1415}f(n) - 2{}^{15}N\sum_{n_{CR}}^{n_P(n_{PI})} K_{CR}\,{}^{1414}f(n)\Bigg]. \quad (40)$$

It is convenient to present the solution of (40) in the form

$$^{14}N(t) + {}^{15}N(t) = \exp\left(-\frac{t}{\tau_A}\right)\Bigg[\int_0^t (^{1414}N_2)^2(^{1415}k_D\beta_{0M} + 2{}^{1414}k_D)\exp\left(\frac{t'}{\tau_A}\right)dt' + {}^{14}N(0) + {}^{15}N(0)\Bigg], \quad (41)$$

$$^{15}N = \exp\left(-\frac{t}{\tau_A} - \int_0^t \frac{dt'}{\tau_{AM}}\right)\Bigg\{\int_0^t \exp\left(\frac{t'}{\tau_A} + \int_0^{t'}\frac{dt''}{\tau_{AM}}\right) \times [Z(t')J(t')]\beta_{0M}dt' + {}^{15}N(0)\Bigg\}, \quad (42)$$

where

$$Z(t') = {}^{1415}k_D(^{1414}N_2)^2 + \exp(-t'/\tau_A)^{1414}N_2 \times \sum_{n_{CR}}^{n_P(n_{PI})} K_{CR}\,{}^{1415}f(n),$$

$$J(t') = \int_0^{t'}(^{1415}k_D\beta_{0M} + 2{}^{1414}k_D)(^{1415}N_2)^2\exp(t''/\tau_A)dt'' + {}^{14}N(0) + {}^{15}N(0),$$

$^{14}N(0)$ and $^{15}N(0)$ — are the concentrations of atoms at the discharge region outlet, and the characteristic atomic–molecular exchange time was introduced:

$$\tau_{AM} = \Bigg[2{}^{1414}N_2\Bigg(\beta_{0M}\sum_{n_{CR}}^{n_P(n_{PI})} K_{CR}\,{}^{1415}f(n) + \sum_{n_{CR}}^{n_P(n_{PI})} K_{CR}\,{}^{1414}f(n)\Bigg)\Bigg]^{-1}. \quad (43)$$

In the case of fast atomic–molecular exchange when

$$\tau_{AM} \ll \tau_A, \tau_M, \quad (44)$$

the solutions of (41), (42) yield the following for the atomic enrichment coefficient:

$$\beta_A(t) = (^{15}N/^{14}N)/(\beta_{0M}/2) \cong \frac{2\left(^{1415}k_D/(2\delta) + \sum_{n_{CR}}^{n_P(n_{PI})} K_{CR}\,{}^{1415}f(n)\right)}{\beta_{0M}\sum_{n_{CR}}^{n_P(n_{PI})} K_{CR}\,{}^{1415}f(n) + 2\sum_{n_{CR}}^{n_P(n_{PI})} K_{CR}\,{}^{1414}f(n)}. \quad (45)$$

Let us compare the terms in the numerator of formula (45). Using relations (4), (8), (9), (15), (20), (21), (34), and (35), one may demonstrate that the ratio of the first term to the second one does not exceed $5 \cdot 10^{-6}/\delta$ within the entire considered range of values of $n_0 \leq 17.5$ at $T = 300$ K. As was already mentioned, the degree of dissociation of molecules in our experiments did not fall outside the $1 \cdot 10^{-4} < \delta < 2 \cdot 10^{-2}$ range; therefore, the first term in (45) may be neglected. Physically, this implies that the direct influence of dissociation of molecules (even those enriched with the heavy isotope) on the coefficient of enrichment of the atomic phase is negligible. The enrichment itself is attributable primarily to the atomic–molecular exchange. In view of this, expression (45) may be transformed into

$$\beta_A \cong \frac{2\sum\limits_{n_{CR}}^{n_P(n_{PI})} {}^{1415}f(n)}{\beta_{0M}\sum\limits_{n_{CR}}^{n_P(n_{PI})} {}^{1415}f(n) + 2\sum\limits_{n_{CR}}^{n_P(n_{PI})} {}^{1414}f(n)} \cong \frac{\sum\limits_{n_{CR}}^{n_P(n_{PI})} \beta_M(n)\,{}^{1414}f(n)}{\sum\limits_{n_{CR}}^{n_P(n_{PI})} {}^{1414}f(n)}. \quad (46)$$

It was taken into account here that $\beta_M(n)\beta_{0M} \ll 2$. If $n_0 \leq n_{CR}$ and $n_I \leq n_{CR}$, the summation over n within the $n_{CR} < n < n_P(n_{PI})$ range is performed at $\beta_M(n) = \text{const}$, and we obtain the following for atomic enrichment coefficient (46):

$$\beta_A \cong \beta_M(n_0), \quad \big(\beta_M(n_I)\big), \quad (47)$$

where $\beta_M(n_0)$ $\big(\beta_M(n_I)\big)$ are defined by expression (21). In accordance with (3), (9), (13), and (15), these conditions persist up to $n_0 = 14$ and $n_I \cong 16$ inclusively. At $15 \leq n_0 \leq 17$ (Fig. 3), $n_I \cong n_{PI} > n_{CR}$, and we write the following relying on (5) and (20):

$$\beta_A \cong \frac{\sum\limits_{n_{CR}}^{n_{PI}} \exp\left[n/5.33 + \big((n-n_0)^2 - n_0^2\big)\gamma E_1/T\right]}{\sum\limits_{n_{CR}}^{n_{PI}} \exp\left[\big((n-n_0)^2 - n_0^2\big)\gamma E_1/T\right]} = \frac{\exp(n_0/5.33)\sum\limits_{n_{CR}-n_0}^{n_{PI}-n_0} \exp(x/5.33 + x^2/14.42)}{\sum\limits_{n_{CR}-n_0}^{n_{PI}-n_0} \exp(x^2/14.42)}. \quad (48)$$

Here, x assumes integer values within the indicated summation limits. Performing summation, we derive a function of n_0 approximating the atomic enrichment coefficient:

$$\beta_A = \exp(0.54n_0 - 4.9), \quad (49)$$

which is easy to sew together at $n_0 = 13.5$ and 14 with functions (21) and (47) for enrichment on the plateau. In order to apply relations (47), (48), and (49) correctly, one needs to verify that condition (44) is satisfied. Let us determine the range of n_0 values within which it is satisfied. If $n_0 \leq 13.5 < n_{CR}$, the summation in (43) is performed in the plateau region, and

$$\tau_{AM} = \left[2^{1414}N_2K_{CR}f^{Tr}(n_0)(n_0+1)(1+\beta_M\beta_{0M})\sum_{n_{CR}}^{n_P}(n+1)^{-1}\right]^{-1} < \left[2^{1414}N_2K_{CR}f^{Tr}(n_0)(n_0+1)/n_{CR}\right]^{-1} < 7 \cdot 10^{-3}\,\text{s}.$$

At $15 \leq n_0 \leq 17$ with the smallness of $\beta_M(n)\beta_{0M}$ taken into account:

$$\tau_{AM} \cong \left[2^{1414}N_2K_{CR}\sum_{n_{CR}}^{n_{PI}} {}^{1414}f(n)\right]^{-1} \cong \left[2^{1414}N_2K_{CR} \times f(0)\exp(-n_0^2/14.42)\sum_{n_{CR}-n_0}^{n_{PI}-n_0}\exp(x^2/14.42)\right]^{-1}. \quad (50)$$

The calculations for $n_0 = 15$, 16, and 17 yield $\tau_{AM} \approx 0.05$, 0.15, and 0.5 s, respectively. The estimates for $\tau_M \approx 0.3$ s, $\tau_A \approx 0.7$ s were obtained above. It can be seen that the maximum value of n_0 at which formula (46) is still applicable is around $n_0 \cong 16$. Atomic enrichment coefficient (49) may then reach a value of $\beta_A^{\max} \cong 42$. Note that atomic–molecular exchange constant K_{CR} itself is not found in expressions (48) and (49) for β_A, but, in accordance with (50), the maximum values of n_0 and n_{PI}, which define the upper limit for the considered approximation, depend on it and on n_{CR}. The similarity between the predicted maximum value of $\beta_A^{\max}$ and the maximum experimental value of $\beta_A^{\max} = 34$ suggests that the values of parameters K_{CR} and n_{CR} used in the present study are accurate. Note also that were it not for the intermediate mode of moderate deviation from equilibrium (and the corresponding regions of inverse population of vibrational levels at $n_0 < n < n_I$), the upper boundary of the plateau would enter region $n_P < n_{CR}$, where the atomic–molecular exchange is infeasible ($\tau_{AM} \to \infty$), already at $n_0 \geq 13.5$ (see Fig. 3), and the atomic enrichment coefficient would not exceed the value of (see (21), (47), and Fig. 4) $\beta_A = \beta_M \leq \exp[(13.5 - 0.675)/5.33] \cong 11 \ll \beta_A^{\max}$.

2.3.3. Analysis of the dependence of the atomic enrichment coefficient on the time of gas flow through the post-discharge zone; comparison with experimental data

The experimental data on the atomic enrichment coefficient in Fig. 1 are presented alongside the approximating curves for $T = 300$ K, $T_{ch} = 400$ K, time $\tau_M = 270$ ms of vibrational energy deactivation on a wall, and different values of the vibrational energy pumping

power per a single molecule, W. These curves were plotted in accordance with Eqs. (21), (47), and (49) with the use of relations (28), (38), and (39). It is evident that the experimental points up to $t \cong 1700$ ms are characterized well (at least qualitatively) by the approximating curves at the indicated deactivation time within the range of pumping power values $W \cong 70-210\,\mathrm{eVs^{-1}mol^{-1}}$. The obtained spread of W values may well be attributable to the specifics of the experimental technique of excitation of vibrational levels with a pulsed voltage generator: as was mentioned above, the calculated total power per a molecule in a discharge varied within the range of $W_T \cong 250-750\,\mathrm{eVs^{-1}mol^{-1}}$ depending on the gas flow velocity and the gas pressure. It can be seen that the relative spread of values of vibrational energy pumping power for molecules determined by approximation and the experimental relative spread of the total discharge power are approximately equal. Note that only about 30% of the discharge power were spent directly on the excitation of vibrations of molecules. Also worth noting is that the obtained characteristic time of deactivation of vibrational energy on a quartz tube wall ($\tau_M = 270$ ms) allows one to estimate independently the probability of vibrational deactivation of nitrogen molecules on this wall (see (24)): $\gamma_M^{\exp} \cong 1.1 \cdot 10^{-4}$. This value is close to the probability used to obtain a preliminary estimate of τ_M: $\gamma_M \approx 1 \cdot 10^{-4}$ [26,27].

As was demonstrated above, the average vibrational energy of a molecule at given power W does, in accordance with (28), pass through maximum at $t = t_{\max} = 0.83\tau_M = 225$ ms (Fig. 5) as the flow time increases. The maximum values of this energy in the considered pumping power range are $\varepsilon_{\max} \cong 0.98-2.94\,\mathrm{eV\,mol^{-1}}$. According to (38), n_0 assumes minimum values within the range of $n_0^{\min} \cong 2.3-6.3$ in this case. The corresponding spread of minimum values of the atomic enrichment coefficient (see (21), (47)) is $\beta_A^{\min} \cong 1.35-2.9$. The trend toward a shallow minimum near these values is visible in Fig. 1 even in the experimental data, although experimental points in the immediate vicinity of $t = 225$ ms are lacking. As the flow time increases to $t \cong 1400-1700$ ms, average vibrational energy ε of molecules decreases, while the values of n_0 (and, consequently, β_A) grow. At $n_0 \cong 16$, β_A approaches the calculated value of $\beta_A^{\max} \cong 42$, passing close to experimental points $\beta_A \cong 21$ and $\beta_A \cong 34$. As the flow time increases further and the values of $n_0 \geq 17$ are reached, characteristic atomic–molecular exchange time τ_{AM} starts exceeding characteristic times τ_M and τ_A. The processes of atomic–molecular exchange become negligible at this point. The direct dissociation of molecules is also negligible. Indeed, it follows from (29), (31), (32), (33), and (34) that the following is true in the considered experimental conditions at $n_0 \cong 17$:

$$\left(\frac{d^{15}N}{dt}\right)_D \ll \left(\frac{d^{14}N}{dt}\right)_D \approx 10^4\,\mathrm{cm^{-3}s^{-1}} \ll 10^{10}\,\mathrm{cm^{-3}s^{-1}}$$

$$< \left|\left(\frac{d^{14(15)}N}{dt}\right)_R\right| = \frac{^{14(15)}N}{\tau_A}$$

(it was taken into account here that the degree of dissociation of molecules of both types is $1 \cdot 10^{-4} < \delta < 2 \cdot 10^{-2}$).

Thus, starting at $n_0 \approx 17$, the recombination of atoms on tube walls becomes the primary process affecting the concentration of atoms in the flow. It follows from (29) and (30) that the additional enrichment due to the difference in mass of isotopes is

$$\beta_{AR} = \exp(t/^{14}\tau_A - t/^{15}\tau_A) = \exp(0.034t/^{14}\tau_A).$$

At $^{14}\tau_A \cong 0.7$ s and time of flow through the post-discharge zone $t = 4.5$ s (the maximum value in our experiments), the additional enrichment does not exceed $\beta_{AR} \cong 1.2$; therefore, the enrichment achieved at the previous stage should be retained with a fairly high accuracy in the proposed model (the weak influence of differences in recombination rates on the ratio of concentrations of atoms of different isotopes allowed us to neglect it in deriving and solving Eqs. (40)). Note that the variables of state of the molecular phase continue to vary with characteristic time τ_M. However, when the time of gas flow becomes close to the longitudinal diffusion time ($t \to \tau_{DL} \approx 8$ s), the considered model is hardly applicable: average vibrational energy of molecules ε and temperature T_1 in a designated gas volume are then defined not only by the interaction of molecules with tube walls at the position of this volume, but also by the mixing with molecules from neighboring regions. This leads to a certain averaging of resulting ε and T_1 and the corresponding enrichment coefficient $\langle\beta_A(t)\rangle < \beta_A^{\max}$. The diffusion mixing of atoms produced in the atomic–molecular exchange with molecules with different ε and T_1 may also reduce the enrichment coefficient. Therefore, the $\beta_A(t)$ dependence should pass both through its minimum and its maximum. These assumptions are verified experimentally: as was indicated above, the observed values of the enrichment coefficient at flow times $t = 2530$ and 4500 ms are equal to $\beta_A = 23.6$ and 7.9, respectively, and are thus significantly lower than the maximum attained value of $\beta_A^{\max} = 34$ at $t = 1667$ (Fig. 1).

Conclusion

Various physical processes possibly contributing to the enrichment of the atomic nitrogen component with isotope ^{15}N in nonequilibrium excited gas flowing along a quartz tube in the post-discharge zone were considered and analyzed. The processes of dissociation of vibrationally excited molecules, atomic–molecular exchange, recombination of atoms, and deactivation of the vibrational energy of molecules on the tube surface were taken into account. A system of differential equations characterizing the dependences of concentrations of ^{14}N and ^{15}N atoms on time t of gas flow through the post-discharge zone in the measurement tube was derived and solved. The special case of fast atomic–molecular exchange with $\tau_{AM} \ll \tau_A, \tau_M$ was considered, and the conditions in which this exchange is implemented for nitrogen were determined. At translational

gas temperature $T = 300\,\mathrm{K}$, the degree of excitation of vibrational levels of molecules should be such that the minimum of the Trinor distribution is positioned no higher than level $n_0 \cong 16$. This corresponds to a vibrational temperature no lower than $T_1 \cong 1556\,\mathrm{K}$ and the conditions of large and moderate deviations from equilibrium. It was demonstrated that the atomic–molecular exchange produces the primary contribution to the enrichment of the atomic component with heavy isotope $^{15}\mathrm{N}$ in these conditions at molecule dissociation degree $\delta > 1 \cdot 10^{-4}$. The high degree of atomic enrichment is due to the activation nature of atomic–molecular exchange: only the nitrogen molecules with high degrees of molecular enrichment located on vibrational levels above a certain critical $n \geq n_{CR} \cong 16.5$ are involved in it. The atomic enrichment coefficient is defined by the average value of the molecular enrichment coefficient on these levels (see (46)).

The expression for atomic enrichment coefficient β_A of nitrogen in the case of fast atomic–molecular exchange was presented in the form of a dependence on number n_0 in the entire allowed range of $n_0 \leq 16$ (see (21),(47),(49)). The dependence of n_0 on average vibrational energy ε of a molecule ((38), (39)) and dependence $\varepsilon(t)$ (28) were determined in order to obtain a time dependence of β_A. Dependence $\varepsilon(t)$ is governed primarily by vibrational energy pumping power W in a discharge and characteristic time τ_M of deactivation of the vibrational energy on the quartz tube surface. Varying these parameters, we obtained a fairly accurate approximation of the experimental data (temporal variation and absolute value) on $\beta_A(t)$ in the region of its applicability (at $n_0 \leq 16$ and $t \leq 1700\,\mathrm{ms}$). This is indicative of the correctness of the proposed model (Fig. 1). The pumping power determined using this approximation allowed us to estimate the fraction of the total discharge power spent directly on the excitation of vibrations of molecules. This was roughly equal to 30%.

Conflict of interest

The authors declare that they have no conflict of interest.

References

[1] M.I. Makarov. Eurasian Soil Sci., **42** (12), 1335–1347 (2009).
[2] R.F. Follett. Commun. Soul Sci. Plant Anal., **32** (7–8), 951 (2001).
[3] H. Förstel. Isot. Environ. Health S., **32** (1), 1 (1996).
[4] Yu.M. Loginov, L.P. Pokhlebkina. In: *Izotopy: svoistva, poluchenie, primenenie*, Ed. V.Yu. Baranov (IzdAT, M., 2000), p. 684 (in Russian).
[5] S.V. Alekseev, V.A. Zaitsev. *Nitridnoe toplivo dlya yadernoi energetiki* (Tekhnosfera, M., 2013) (in Russian).
[6] V.I. Rachkov, E.O. Adamov. *Proc. Ind. Conf. „Closure of the Nuclear Fuel Cycle on the Basis of Fast Neutron Reactors"* (Tomsk, Russia, 2018), p. 6 (in Russian).
[7] C.E. Treanor, J.W. Rich, R.G. Rehm. J. Chem. Phys., **48** (4), 1798 (1968).
[8] B.F. Gordiets, S. Zhdanok. In: *Nonequilibrium vibrational kinetics*, ed. by M. Capitelli (Springer-Verlag, Berlin, Heidelberg, 1986), p. 47–84.
[9] M. Cacciatore, M. Capitelli, S. De Benedictis, M. Dilonardo, C. Gorse. In: *Nonequilibrium vibrational kinetics*, ed. by M. Capitelli (Springer-Verlag, Berlin, Heidelberg, 1986), p. 5–46.
[10] B.F. Gordiets, Sh.S. Mamedov. Sov. J. Quant. Electron., **5** (9), 1082 (1975).
[11] E.M. Belenov, E.P. Markin, A.N. Oraevskii, V.I. Romanenko. JETP Lett., **18** (3), 116 (1973).
[12] V. Kudrle, A. Tálský, J. Janča. *Proc. of XXIV–ICPIG* (Warsaw, 1999), **1**, p. 167.
[13] N.M. Gorshunov, S.V. Gudenko. JETP Lett., **77** (4), 162 (2003).
[14] V.M. Akulintsev, N.M. Gorshunov, Yu.P. Neshchimenko. Khim. Vys. Energ., **15** (2), 165 (1981) (in Russian).
[15] B.T. Baísova, S.L. Dolganeva, V.I. Strunin, N.N. Strunina, I.A. Tikhomirov. Tech. Phys., **46** (5), 529 (2001).
[16] V.I. Strunin, N.N. Strunina, B.T. Baisova. Tech. Phys., **51** (2), 163 (2006).
[17] D.I. Slovetskii. *Mekhanizmy khimicheskikh reaktsii v neravnovesnoi plazme* (Nauka, M., 1980) (in Russian).
[18] M. Tinkham, M.P. Strandberg. Phys. Rev., **97** (4), 937 (1955).
[19] S. Krongelb, M.P. Strandberg. J. Chem. Phys., **31** (5), 1196 (1959).
[20] G.D. Billing. In: *Nonequilibrium vibrational kinetics*, ed. by M. Capitelli (Springer-Verlag, Berlin, Heidelberg, 1986), p. 85–112.
[21] G.D. Billing, E.R. Fisher. Chem. Phys., **43** (3), 395 (1979).
[22] A. Lofthus, P.H. Krupenie. J. Phys. Chem. Ref. Data, **6** (1), 113 (1977).
[23] Sh.S. Mamedov. Tr. FIAN, **107**, 3 (1979) (in Russian).
[24] A.A. Likalter, G.V. Naidis. Chem. Phys. Lett., **59** (2), 365 (1978).
[25] M. Capitelli, C. Gorse, A. Ricard. In: *Nonequilibrium vibrational kinetics*, ed. by M. Capitelli (Springer-Verlag, Berlin, Heidelberg, 1986), p. 315–337.
[26] V.A. Shakhatov, O.A. Gordeev. Tech. Phys., **50** (12), 1592 (2005).
[27] V.P. Zhdanov, K.I. Zamaraev. Catal. Rev., **24** (3), 373 (1982).
[28] I.N. Brovikova, E.G. Galiaskarov. High Energ. Chem., **37** (5), 341 (2003).
[29] B.E. Zhestkov, S.N. Kozlov, E.N. Alexandrov. High Temp., **57**, 329 (2019).